NanoImpact 26 (2022) 100397

Contents lists available at ScienceDirect

NanoImpact

journal homepage: www.elsevier.com/locate/nanoimpact

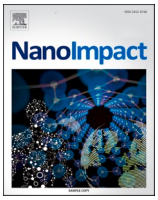

Similarity assessment of metallic nanoparticles within a risk assessment framework: A case study on metallic nanoparticles and lettuce

Yuchao Song [a,*], Eric Bleeker [b], Richard K. Cross [c], Martina G. Vijver [a], Willie J.G.M. Peijnenburg [a,b]

[a] Leiden University, Institute of Environmental Sciences (CML), P.O. Box 9518, 2300, RA, Leiden, the Netherlands
[b] National Institute of Public Health and the Environment (RIVM), Centre for Safety of Substances and Products, P.O. Box 1, Bilthoven, the Netherlands
[c] UKRI Centre for Ecology and Hydrology, MacLean Building, Benson Lane, Wallingford OX10 8BB, UK

ARTICLE INFO

Editor: Bernd Nowack

Keywords:
Nanoparticles
Toxicity
Lettuce
Grouping
Similarity assessment
Risk assessment

ABSTRACT

Similarity assessment is one of the means of optimally using scarcely available experimental data on the fate and hazards of nanoforms (NFs) for regulatory purposes. For a set of NFs that are shown to be similar it is allowed in a regulatory context to apply the information available on any of the NFs within the group to the whole set of NFs. Obviously, a proper justification for such a similarity assessment is to be provided. Within the context of exemplifying such a justification, a case study was performed aimed at assessing the similarity of a set of spherical metallic NFs that different with regard to chemical composition (three metals) and particle size (three different sizes). The endpoints of assessment were root elongation and biomass increase of lettuce (*Lactuca sativa L.*) seedlings and exposure assessment was performed in order to express the actual exposure concentration in terms of time-weighted average particle concentrations. The results of the study show that for the specific endpoints assessed, chemical composition is driving NF toxicity and this is mostly due to impacts on the fate of the NFs. On the other hand, particle size of Cu NFs had a negligible impact on the dose-response relationships for the specific endpoints assessed. It is thus concluded that hazard data available on spherical Cu NF tested in our case can be used to inform on the hazards of any spherical Cu NF within the size range of 25–100 nm, but only applies for the certain endpoints. Also, toxicity data for the Cu^{2+}-ion are suited for such a similarity assessment.

1. Introduction

Numerous nanomaterials with unique characteristics have been applied in a large variety of medical, industrial and environmental applications (Simeone et al., 2019; Sizochenko et al., 2021). Chemical risk assessment is typically lagging behind materials innovations. However, given the current pace of innovation of nanomaterials it is essential for adequate risk assessment to incorporate as efficiently as possible all kinds of information available regarding the fate and hazards of nanomaterials. Efficient use of information is also required in view of the general desire to minimize animal testing for regulatory purposes. One of the tools that can be employed for efficient risk assessment of nanomaterials, is to use as efficiently as possible all information available for similar nanomaterials. For instance, Annex VI, section 2.4 of the European regulation for chemical risk assessment (REACH) indicates that a nanoform (NF) shall be characterized in accordance with REACH (European Commission, 2018). Any substance may have one or more NFs, based for instance on differences in their number-based particle size distribution, size, shape, aspect ratio, or crystallinity. For a set of NFs that are shown to be similar it is allowed to conclude that the hazard assessment, exposure assessment, and risk assessment of these NFs can be performed jointly. This implies that all information available on any of the NFs within the group, can be applied to the whole set of NFs. A justification shall be provided to demonstrate that a variation within the boundaries defined for the set of NFs does not affect the hazard assessment, exposure assessment and risk assessment of the similar NFs in the set. It is to be noted that the similarity assessment may consist of using the same data obtained for one or more of the NFs in the group for the whole group of NFs. It is also possible to apply validated relationships between any of the properties of the NFs and their fate or toxicity parameters to estimate missing properties of some of the NFs in the set of NFs. Up till now, limited experience has been gained regarding similarity assessment of NFs and this prompted us to perform a case study on similarity assessment of a set of spherical metallic NFs differing in size

* Corresponding author.
E-mail address: y.song@cml.leidenuniv.nl (Y. Song).

https://doi.org/10.1016/j.impact.2022.100397
Received 14 March 2022; Accepted 17 March 2022
Available online 25 March 2022

and in chemical composition. Given the ease of testing, hydroponic exposure of lettuce (*Lactuca sativa L.)* was selected as the endpoint of interest to exemplify the case. Specific attention was paid to the fate assessment of the NFs with specific focus on quantifying the kinetics of release of metal ions shed from each of the NFs and on assessing the time-dependent contribution of particles and released ions to overall suspension toxicity.

Extensive safety research within the last decade on nanomaterials has improved the database and the knowledge on the effects of engineered nanoparticles (NPs) on plants (Abbas et al., 2020; Zhu et al., 2019). It nevertheless is still unknown how the different physicochemical properties (e.g., size, shape, and surface chemistry) of NPs and the various experimental conditions (e.g., various exposure pathways) actually affect nanotoxicity (Pedruzzi et al., 2020; Zhai et al., 2017). The physicochemical properties of NPs and the experimental conditions also determine the fate of NPs in the aqueous environment. As discussed by Peijnenburg et al. (2015), the key processes governing the fate of metallic NPs in aquatic media are dissolution, and aggregation and subsequent sedimentation. A plethora of particle-specific and media-specific variables affect the dissolution profile of NPs (e.g. particle composition, particle size, pH, natural organic matter, temperature) and these variables can be spatially and temporally highly heterogeneous (Hedberg et al., 2019). To avoid extensive toxicological testing of each single nanomaterial, it is becoming increasingly important to group or categorize these NPs (Arts et al., 2014; Ban et al., 2018), whilst avoiding the media-specific on the fate of the NPs to cloud the overall picture of similarity of NFs. Cu NPs have been incorporated as additives in lubricants, polymers, and inks (Adeleye et al., 2014; Conway et al., 2015). Because of their small size and ability to release ions especially in acidic conditions, Cu NPs have antimicrobial properties and have been proposed as additives to traditional wastewater treatment systems (Chen et al., 2006). As reported, the solubility of Cu and ZnO nanoparticles in various environmentally relevant media is determined to be in the range of 1–80% during exposure periods ranging from 5 min to 48 h, which highlights the importance of thorough and exposure-specific characterization of the fate of the NPs during experiments (Misra et al., 2012).

Although there is a vast amount of literature on the potential impact of NPs on plants (Sturikova et al., 2018; Song et al., 2020), the majority of papers have reported the impact of NPs only at an early stage of plant development, mainly addressing the effects of NPs on seed germination and root elongation (Konate et al., 2018; Lv et al., 2021; Pu et al., 2019; Velicogna et al., 2020). Thus, a better knowledge of the effects of NPs on plants at a later stage of plant development is needed, for instance during a longer period of exposure and by means of additional observations of biomass changes. This study aims to: 1) investigate the impact of particle composition, size and initial concentration on the dissolution profile of metallic NPs, 2) determine long term effects of NPs on the root elongation and growth (biomass production) of lettuce, 3) to quantify the impacts of chemical composition and particle size on toxicity. We hypothesize that higher ion release will occur for lower-sized NFs whereas ionic toxicity is expected to dominate the toxicity of NPs suspensions. We finally hypothesize that there is a relationship between particle toxicity and particle size, which can be used as the basis for similarity assessment of NFs. To this end, we selected five spherical metal-based NPs (three Cu NPs of different size, one ZnO NP of similar nominal size as one of the Cu NPs (25 nm) and one $BaSO_4$ NP of similar nominal size (100 nm) as one of the Cu NPs), evaluating their effects on plant growth by assessing relative root elongation and biomass change during exposure of up to 20 days to various particle concentrations with exchange of the exposure medium every 2 days. The toxicity profile of the corresponding metal ions was assessed as well in order to allow for assessing the contribution of the particles to the overall suspension toxicity.

2. Materials and methods

2.1. Preparation and characterization of NPs suspensions

Spherical Cu NPs with nominal particle diameters of 25 nm (uncoated nanospheres, coded NM-0016, purity 99.5%) and 60–80 nm (uncoated nanospheres, coded NM-0044, purity 99.9%), and 100 nm Cu NPs (uncoated nanospheres, purity 99.9%) were purchased from the US Research Nanomaterials, Inc. (Houston, TX USA). ZnO NPs (uncoated nanospheres, coded NM-110, purity 99%) with nominal size of 25 nm, were purchased from the Io-Li-Tec company (Heilbronn, Germany) and 100 nm $BaSO_4$ NPs (uncoated nanospheres, coded NM-220, purity 99.9 m %) were obtained from the Joint Research Centre of the European Union (Ispra, Italy). $Cu(NO_3)_2{\cdot}2H_2O$ (purity 99%), $Zn(NO_3)_2{\cdot}6H_2O$ (purity 99.5%) and $BaCl_2{\cdot}2H_2O$ (purity 99%) used in the experiments were all purchased from the Merck KGaA company (Darmstadt, Germany). The morphology and size of the tested metallic nanoparticles were characterized by using transmission electron microscopy (TEM, JEOL 1010, JEOL Ltd., Japan). The size distribution and zeta potential of the nanoparticle suspensions at 10 mg L^{-1} were analysed after 0.5, 24 and 48 h of incubation in 1/4 Hoagland solution by a Zetasizer Nano-ZS instrument (Malvern, Instruments Ltd., Royston, UK). Aliquots from the solid Cu NPs were always taken under an argon atmosphere to prevent oxidation of the particles. Stock suspensions of the NPs were freshly prepared in 1/4 Hoagland solution (pH 6.0 ± 0.1) after 30 min of sonication at 60 Hz (USC200T, VWR, Amsterdam, the Netherlands). The composition of the Hoagland medium is given in Table S1 of the Supplementary Information. The dissolution kinetics of the suspensions of the NPs at each concentration were investigated to obtain the actual exposure concentrations of soluble ions and particles. After being exposed to 1/4 Hoagland solution for 0.5, 2, 4, 8, 24 and 48 h in a 22 mL glass tubes, five mL of suspension (defined as NPs (total)) were firstly sampled from the middle of the tube, making sure that the tip was always fixed at the middle part of the suspension left in the tube. Fifteen mL of suspension were sampled and centrifuged for 30 min at 30,392*g* and at 20 °C (Sorvall RC5Bplus centrifuge, Bleiswijk, Netherlands) to remove the particles. The obtained supernatants of the NPs were analysed to obtain the concentration of ions released from the NPs in suspension (defined as NPs(ion)). Next, the concentrations of NPs (total) and NPs (ion) were measured by means of Atomic Absorption Spectroscopy (AAS, PerkinElmer 1100 B, Waltham, MA, USA) after addition of a drop of 65% HNO_3 into the solution. All experiments were performed in triplicate.

2.2. Plants culture and toxicity test

L. sativa L seeds were purchased from Floveg GmbH (Kall, Germany) and sterilized for 15 min with NaClO (0.5% *w/v*), rinsed three times with tap water, and then immersed in deionized water for germination. After 4 days, the seedlings with taproot length in the range of 2–3 cm were chosen and put in Petri dishes containing 30 mL of 1/4 Hoagland solution. Four seedlings were cultured in each Petri dish. The seeds germination and the exposure to the NPs were performed in a climate room at a 25/16 °C day/night temperature and 60% relative humidity, at a 16 h photoperiod. The relative root elongation (RRE) and biomass production were determined as the toxicological endpoints which are sensitive to the impacts of external stressors (Liu et al., 2016). The nominal concentrations of the three sizes of Cu NPs ranged from 0.01 to 0.2 mg L^{-1}, the concentrations used for the ZnO NPs ranged from 0.2 to 20 mg L^{-1}, the range of $Cu(NO_3)_2{\cdot}2H_2O$ was from 0.01 to 2 mg L^{-1}, and the range of concentrations of $Zn(NO_3)_2{\cdot}6H_2O$ tested was from 0.1 to 4 mg L^{-1}. $BaSO_4$ NPs were tested at concentrations ranging from 800 to 1000 mg L^{-1}. In order to determine the toxicokinetics of the impacts of the NPs, the exposure period was prolonged to 20 days. The medium was refreshed once every 48 h. Just before each medium refreshment the taproot length was measured by a ruler (0.1 cm accuracy) from the

transition point between the hypocotyls and the root to the root tip. The root growth of each treatment was defined as the mean value of the differences in root length of four seedlings before and after each exposure. RRE was determined according to eq. 1:

$$RRE = \frac{R_{Gs}}{R_{Gc}} \times 100\% \quad (1)$$

RG_s: the root growth of plants in the sample solution, cm;
RG_c: the root growth of plants in the control solution, cm.

The fresh biomass of seedlings was determined after the seedlings were dried by blotting a couple of times with a soft tissue. Plant were confirmed as being dead seedlings and disposed of once the biomass did not change after 48 h. The increase of biomass was calculated according to eq. 2:

$$Biomass\ increase = \frac{MG_c - MG_s}{MG_c} \times 100\% \quad (2)$$

MG_s: the fresh biomass of plants in the sample suspension (gram);
MG_c: the fresh biomass of plants in the control solution (gram).

The behaviour of NPs in aquatic exposure systems is highly dynamic with the actual exposure concentrations of NPs as well as of their transformation products (in the case of metallic NPs being ions released from the particles) varying over time. To account for the dynamics of exposure, time-weighted average concentrations (C_{TWA}) were determined to assess the actual exposure concentration of NPs (total), NPs (particle) and NPs(ion) during each refreshment period of 48 h. The TWA concentration was calculated based on the following equation (Zhai et al., 2016):

$$C_{TWA} = \frac{\sum_{n=0}^{N}\left(\Delta t\ \frac{C_{n-1}+C_n}{2}\right)}{\sum_{n=1}^{N}\Delta t_n} \quad (3)$$

where Δt was the time interval, n is the time interval number, N is the total number of intervals ($N = 10$), C is the concentration at the end of the time interval.

The response addition model was selected to calculate the relative contribution of NPs (particle) and NPs (ion) to the effects on root elongation and biomass induced at a specific suspension concentration of NPs. Based on previous literature (Liu et al., 2016), it is acknowledged that the modes of action of metallic nanoparticles and metal ions are likely to be different, which is the basis for the application of the response addition model:

$$E_{total} = 1 - \left[\left(1 - E_{particle}\right)\left(1 - E_{ion}\right)\right] \quad (4)$$

where E(total) and E(ion) represent the effects caused by the nanoparticle suspensions and their corresponding released ions. In this study, E(total) was measured by the RRE and biomass increase experimentally; E(ion) was calculated according to the dose-response curve of Zn $(NO_3)_2{\cdot}6H_2O$ and $Cu(NO_3)_2{\cdot}2H_2O$ towards impacts on RRE and biomass increase. Therefore, the toxic effects caused by the particles (E(particle)) can be calculated directly by means of eq. 4. The dose-response models were calculated using GraphPad Prism 8.0 and the EC_{50} values for the total and the particulate forms of NPs were subsequently determined.

2.3. Data analysis

Statistically significant differences between different exposure concentrations of the same NP were analysed by means of one-way ANOVA followed by Turkey's honestly significant difference tests at $\alpha < 0.05$ using IBM SPSS Statistics 25. The t-test was performed to analyse the statistically significant differences between NPs (ion) and NPs (total) ($p < 0.05$). Results are expressed as mean ± standard error of 3 replicates.

3. Results

3.1. Physico-chemical characterization of the NPs

The transmission electron microscopic images of the differently sized NPs of different composition in the 1/4 Hoagland solution are shown in Fig. S1 of the Supplementary Information. Data on size distribution and zeta potential after 0 or 0.5, 24 and 48 h of incubation in the 1/4 Hoagland solution of all NPs are given in Table 1. The TEM images confirmed that the particles used in this study were approximately spherically shaped. After being dispersed in the 1/4 Hoagland solution, the particles were present largely as aggregates and the size of the aggregates increased dramatically during 48 h of exposure. Extensive sedimentation of $BaSO_4$ nanoparticles was visible after the suspension was prepared while sedimentation of Cu/ZnO NPs was not observed in any of the samples.

3.2. Dissolution profile of the five NPs studied

The concentrations of the Cu ions released from the Cu NPs within 48 h of exposure are shown in Figs. 1a - 1d. Up to about 85% of the Cu particles dissolved after 48 h of exposure and the ionic copper concentration generally reached a plateau after 8 h of exposure. The overall trend observed was that dissolution occurred at the highest rate in the first two times intervals (0–2 and 2–4 h). The relative amounts of dissolved Cu ions were different for the differently sized Cu NPs, with 0.1 mg L^{-1} 25 nm Cu NPs releasing more Cu ions (94.9%), whereas 87% of Cu ions were released from the 100 nm Cu NPs after 48 h exposure at the same initial exposure concentration (Fig. 1c). However, there was no significant difference of the percentage of ion release between different concentrations of NPs for the same sized particles ($p < 0.05$). The only exception was the 100 nm Cu NPs at an initial concentration of 0.01 mg L^{-1} as about 98% of these particles were dissolved after 48 h of exposure, which was even higher than at a similar concentration of the 25 nm NPs (89% dissolved).

The dissolution profiles of the ZnO NPs, as provided in Fig. 2a illustrated that 81% of the particles were dissolved after 0.5 h of exposure at each concentration tested. The solubility of the ZnO NPs was around 90% after 48 h of exposure, except for the highest concentration tested of 20 mg L^{-1}. When compared with the 25 nm Cu NPs present at the same concentration, especially in the first few hours of exposure considerable differences between the dissolution profiles of the particles were observed (as illustrated in Fig. 2b). As stated above, the 0.2 mg L^{-1} suspension of ZnO NPs was dissolved for 81% after 0.5 h of exposure while only 30% of the Cu NPs were dissolved after this exposure time. Also, the steady state concentration of the ZnO NPs was reached already after 4 h of exposure while it took 8 h for the Cu NPs to reach their steady state level (Fig. 2b).

Table 1
Hydrodynamic diameter and zeta potential of the tested metallic NPs during 48 h of incubation.

Composition	Size (nm)	Hydrodynamic diameter (nm)[a]			Zeta potential (mv) [a]	
		0.5 h	24 h	48 h	0 h	48 h
Cu	25	1259 ± 119	1509 ± 179	1955 ± 269	−0.8 ± 0.3	−0.7 ± 0.4
	60–80	1168 ± 103	1748 ± 19	2015 ± 28	−0.4 ± 0.3	−1.6 ± 0.3
	100	909 ± 67	1191 ± 91	1772 ± 179	−0.4 ± 0.2	1.4 ± 0.4
ZnO	25	1630 ± 232	1718 ± 251	1901 ± 200	−10.3 ± 0.2	−9.0 ± 1
$BaSO_4$	100	96 ± 6	875 ± 147	7457 ± 1478	−15.1 ± 1	−17 ± 1

[a] Hydrodynamic diameter and zeta potential are expressed as the mean ± standard deviation (n = 3).

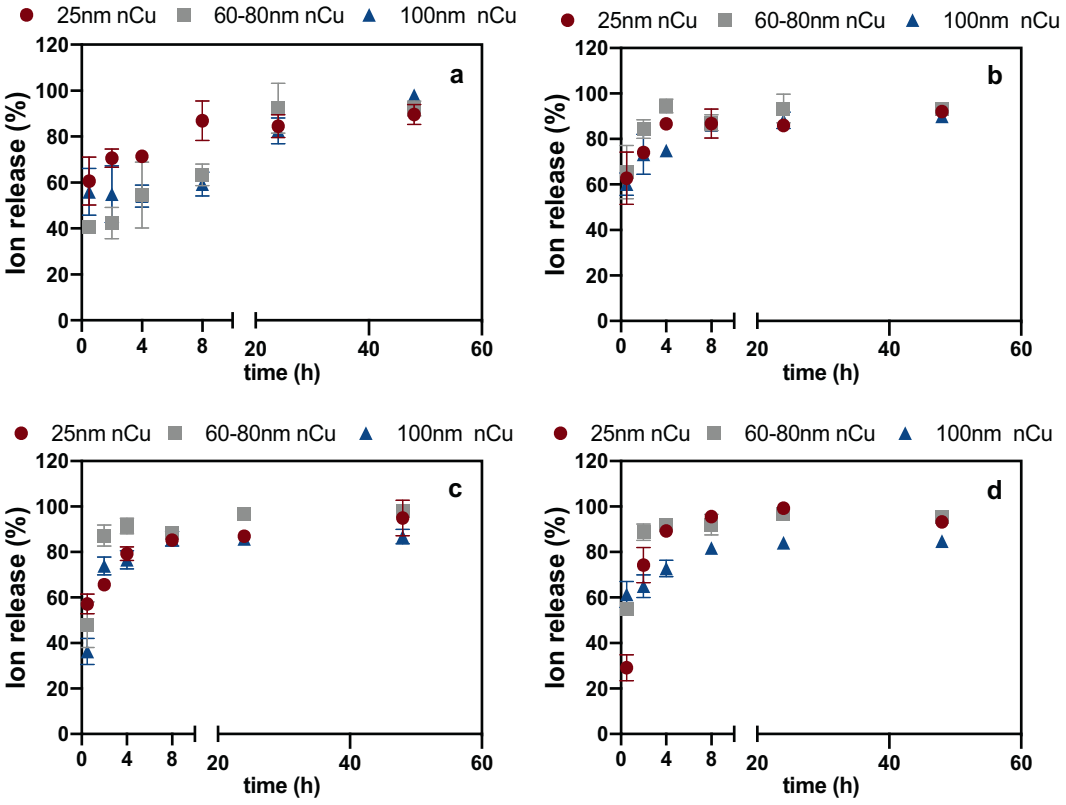

Fig. 1. Percentage of dissolved Cu released from Cu NPs suspensions. of Cu NPs suspensions during 48 h in the exposure medium at each concentration: (a) 0.01 mg L^{-1}; (b) 0.02 mg L^{-1}; (c) 0.1 mg L^{-1}; (d) 0.2 mg L^{-1}. Data are expressed as the mean ± SD (n = 3).

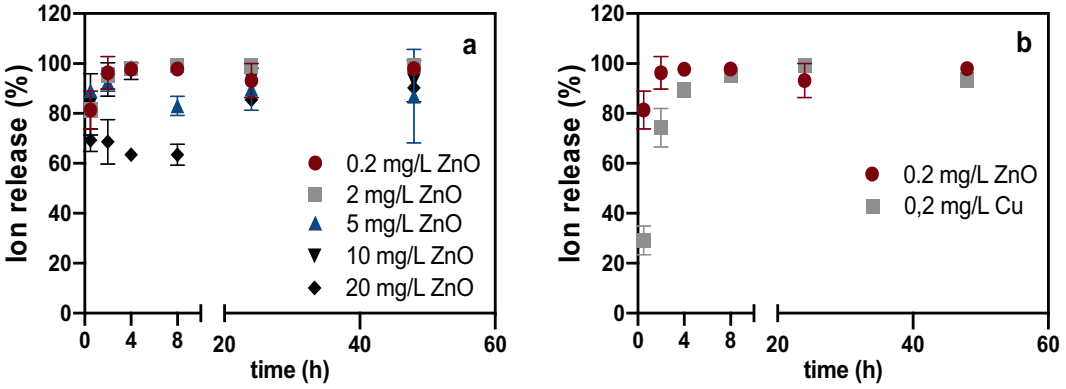

Fig. 2. Percentage of ion release from ZnO NPs suspensions during 48 h of exposure at different initial concentrations (a). Comparison of the ion release profiles of spherical ZnO and Cu NPs of similar size of 25 nm and at the same exposure concentration (b). Data aree expressed as the mean ± SD (n = 3).

The key observation for the 100 nm $BaSO_4$ NPs was that they hardly dissolve and very quickly sediment, with initially (as shown in Table 1) only a small amount of non-aggregated particles remaining after 0.5 h of exposure. Because of their very low solubility, $BaSO_4$ NPs were tested at the highest exposure concentrations amongst the five particles tested in this study. According to the results shown in Fig. 3, the lowest percentage of ion release of all particles tested was observed in the case of $BaSO_4$ NPs: only 7 mg L^{-1} of Ba ions were found to be present at an initial concentration of 1000 mg L^{-1} when the suspensions were freshly made (i.e. with the determination of the actual concentrations of particles and ions performed after 0.5 h) while the remaining concentration of Ba left in suspension was 414 mg L^{-1} after 0.5 h (Fig. 3b). The exposure time was prolonged from the maximum of 48 h as used for the other NPs to 15 days in order to investigate whether the solubility of $BaSO_4$NPs increases after a longer exposure period. However, the concentration of Ba remained low at values in between 0.17 and 0.9 mg L^{-1} at all extended timepoints (Fig. 3). Overall, fast aggregation followed by sedimentation is the dominant process determining the fate of $BaSO_4$ NPs in Hoagland solution. Comparing the fate of the Cu and $BaSO_4$ NPs of 100 nm nominal size thus clearly shows that chemical composition is a key property determining the fate of the NPs in aquatic suspensions.

3.3. *Toxicity profiles of the metallic NPs*

The RRE and the impacts of ions and NPs on biomass production of lettuce as compared to the control were used as the endpoints of toxicity assessment during an overall test duration of 20 days with refreshment of the exposure suspensions or of the ion solutions every 48 h. The

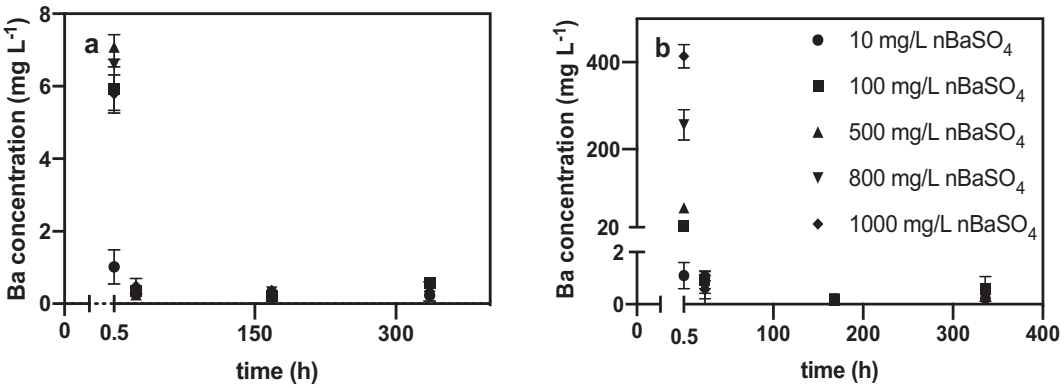

Fig. 3. Concentration of dissolved Ba-ions (a) and total Ba (b) as determined in suspensions of different initial concentrations of $BaSO_4$ NPs during 336 h of exposure. Data were mean ± SD ($n = 3$).

responses of the plants were recorded at each renewal of the medium. Thus, every two days the dose-response curves of the suspensions of the NPs were obtained. Based on the measured total exposure concentrations and the ion release profiles of the NPs, the exposure concentrations of the NPs and the EC_{50} of both suspensions and particulate forms (eq. 4) during 480 h of incubation were determined as based on the time-weighted average exposure concentrations.

3.4. Toxicity of ZnO NPs and $Zn(NO_3)_2{\cdot}6H_2O$ after 480 h of exposure

As indicated above, the ZnO NPs of 25 nm size dissolved very quickly in the ¼ Hoagland medium with in general over 80% of the particles being dissolved within 0.5 h of exposure. Given the high rates of dissolution, the toxicity of the suspensions was fully dominated by the toxicity of the Zn^{2+}-ions released from the particles with EC50-values for both particle suspensions and ion solutions equal to 0.5 mg L^{-1}. Thus, no particle specific impacts were observed.

3.5. Toxicity of $BaSO_4$ NPs and Ba^{2+}-ions

Exposure concentrations of up till 1000 mg L^{-1} of the 100 nm $BaSO_4$ NPs and of Ba^{2+}-ions in the ¼ Hoagland medium did not induce any adverse effects on either root elongation or on biomass formation. As shown above, sedimentation is the key fate process governing the fate of $BaSO_4$ NP in the medium. This implies that the actual exposure concentration of the lettuce roots to the NPs is very low with a maximum concentration of Ba measured in the medium after about 0.5 h of exposure. Similarly, in case of exposure to Ba^{2+}-ions ($BaCl_2$) it is the low solubility limit of the salt that is limiting actual exposure of the roots and protects the plants from adverse effects.

3.6. Toxicity of Cu NPs and Cu^{2+}-ions

The overall finding was that root elongation as well as biomass production were effected by either the Cu-ions or the NP suspensions at concentrations in between 0.01 and 0.1 mg L^{-1}. Clear dose-response relationships were observed, as depicted in Figs. 4 (RRE) and 5 (increase of biomass). Table 2 provides an overview of the actual exposure ranges as based on the measured C_{TWA} of each of the Cu NPs and the Cu^{2+}-ions. Thereupon, the EC_{50}-values as determined for the NP suspensions, the Cu^{2+}-ion, and the Cu NPs (eq. 4) are shown in Table 2 for the endpoints root elongation and biomass production. In case of root

Table 2
The EC_{50} values of the total and particulate forms of Cu NPs and Cu ions as calculated using the RA model (eq. 4). The EC_{50} values are expressed in terms of the time weighted average Cu concentration (C_{TWA}) of either the Cu NP suspensions ($NP_{(total)}$) or of the particulate form of the Cu NPs ($NP_{(particulate)}$) after 480 h of exposure with 10 medium refreshments.

NPs	Exposure range (mg L^{-1})	EC_{50} (mg L^{-1})			
		Cu $NP_{(total)}$		Cu $NP_{(particulate)}$	
		RRE	Biomass increase	RRE	Biomass increase
25 nm Cu NPs	0.01–1.30	0.03	0.03	0.01	0.02
60–80 nm Cu NPs	0.02–0.89	0.04	0.06	0.02	0.03
100 nm Cu NPs	0.01–0.31	0.02	0.10	0.01	0.03
Cu^{2+}	0.01–1.80	0.07	0.06	/	/

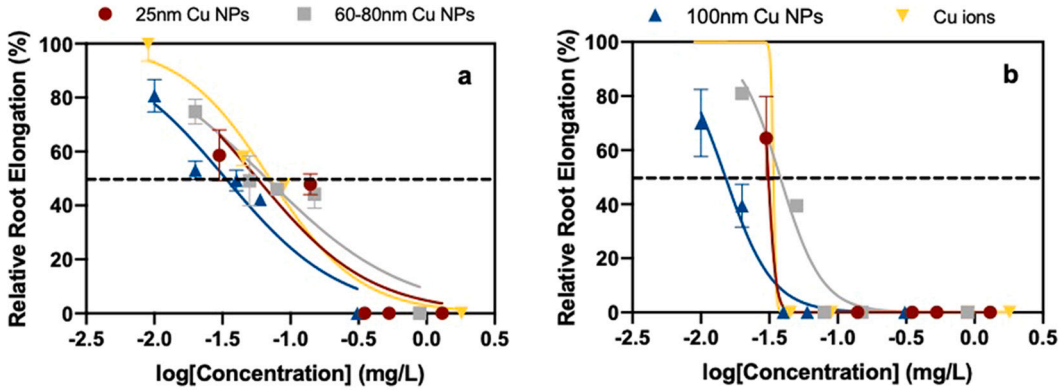

Fig. 4. Dose-response curves of RRE of *Lactuca sativa* L exposed to suspensions of Cu $NPs_{(total)}$ and solutions of $Cu(NO_3)_2{\cdot}2H_2O$ for 144 (a) and 480 h (b) of exposure. Exposure concentrations are expressed as the time weighted average concentrations. Data represent the mean ± SD (n = 3).

elongation as the endpoint, the EC_{50} values for $Cu(NO_3)_2{\cdot}2H_2O$ was 0.07 mg L^{-1} Cu^{2+}. An EC_{50}-value of 0.06 mg L^{-1} Cu^{2+} was obtained for biomass decrease. These values do not differ significantly and it is thus to be concluded that both endpoints were equally sensitive for exposure to Cu^{2+}-ions. The EC_{50}-values of the particulate forms of the three Cu NPs as obtained using the response addition model (RA) are in the range of 0.01–0.03 mg L^{-1} and similar to eh case of Cu^{2+}-ions both endpoints assessed in this study are equally sensitive to exposure to NPs of different size. The EC_{50}-values of the Cu NPs are slightly below the EC_{50}-values of the ions. However, the differences are not statistically significant. There is also no statistically significant difference in toxicity across the three Cu NPs of different size.

Figs. 4 and 5 represent the dose-response curves obtained after 144 and 440 h of exposure. In Fig. 6 the dynamics of the ion and NP suspensions are displayed, showing the EC_{50}-values as a function of exposure time for both endpoints assessed in this study. When the endpoint was RRE, all EC_{50}-values achieved steady state after 288 h of exposure, the suspension of the 100 nm Cu NPs had the lowest EC_{50} (0.02 mg L^{-1}) and the suspension of the 60–80 nm Cu NPs was the least toxic (EC_{50} = 0.04 mg L^{-1}). In general, slightly higher EC_{50}-values were obtained for the endpoint of biomass increase. For this endpoint too, the EC_{50}-values remained the same after 288 h of exposure, except for some small deviations for the the Cu^{2+}-solutions.

4. Discussion

The results of this study showed that especially the chemical composition of NPs significantly affects lettuce root elongation and biomass increase, whereas particle size has a virtually negligible effect on these endpoints. These findings are to a major extent the consequence of the processes determining the fate of the NPs ion the test medium selected. Especially the pH value of 6 of the Hoagland medium strongly affects the kinetics of dissolution of the ZnO NPs as well as the Cu NPs and it is to expected that a higher pH would reduce the rate of dissolution, as discussed by Hortin et al. (2020). This would in turn increase the time weighted average particle concentrations and the potential for more significant contributions to suspension toxicity. The focus of our study was on the time-resolved actual exposure concentrations of ions and particles in suspension. These were quantified separately as a function of exposure duration. As non-dissolved or non-suspended cannot interact with the roots of the lettuce plants, the sedimented particles were not specially quantified. However, as it is impossible to 'loose' metal over the duration of the experiment, and thus the concentration of sedimented metal can be calculated based on the data provided in Table 1 and in the Figures reflecting the time-course of the concentrations of ions and particles in suspension.

Given the observed pattern of Cu^{2+}-ions being slightly less toxic than the Cu NPs used in this study, it is likely that overall suspension toxicity increases at higher pH. On the other hand, the fate and the (lack of) toxicity of the $BaSO_4$ NPs were driven by fast particle aggregation kinetics and subsequent fast sedimentation. Particle aggregation is known to be strongly affected by the ionic strength of the medium (Baalousha et al., 2016) with rates of aggregation decreasing at decreasing ionic strength. However, it is unlikely that reduction of the ionic strength of the Hoagland medium whilst maintaining the minimum amounts of nutrients needed to sustain growth of the lettuce plants, would sufficiently reduce aggregation of the $BaSO_4$ NPs in order to observe any adverse impacts on growth of the lettuce seedlings.

Particle dissolution is affected by the physico-chemical characteristics of NPs, e.g. shape, size, and initial concentration (Angel et al., 2013). It has been reported that dissolved Cu^{+}-ions released by Cu NPs are readily oxidized to Cu^{2+} ions and then complexed in the environment (Adeleye et al., 2014; Lin et al., 2018). This provides the driving force for continued release of Cu^{2+} ions and accounts for the relatively high ion release that was observed. The key issue is on the method used to separate ions and particles. In one of our publications, using metallic nanoparticles in a similar medium, we confirmed that the conditions used for centrifugation of the suspensions provide an effective method to reliably obtain the concentrations of released ions from NPs, achieving fully similar results as compared to results of membrane-based filtration (Xiao et al., 2015). Here we assessed NPs differing in dissolution potential, with the ZnO NPs being more soluble than the NPs of a different chemical composition. The results of Xiao et al. (2015), as obtained in a different exposure medium, indicated that the differences in the extent of dissolution of Cu NPs and ZnO NPs were related mainly to their initial concentration, in which the equilibrium between truly dissolved metal ions, complexed ions, and metal ions absorbed on the remaining particles influenced the overall rate of ion release. In our case, the initial concentrations of Cu NPs did not exert any effect on the extent of dissolution of the particles. It is common practice in regulatory research to mimic realistic environmental conditions. Amongst others this is needed as the composition of the aquatic environment fluctuates strongly over time and space. The conditions employed in this study reflect conditions that are within the ecological boundaries of the lettuce plants used. The experimental design was such that it allowed to verify our hypothesis and we would like to stress that this experimental design can be directly applied to any aquatic medium as the experimental design combines proper fate assessment with proper impact assessment of particles and ions. Toxicity studies with NPs of different composition, size and shape, have been performed on a variety of ecologically relevant species (Arenas-Lago et al., 2019; Wu et al., 2020a, 2020b; Zhai et al., 2019).

Our results showed that the root growth and fresh biomass production of lettuce plants were inhibited after exposure to Cu NPs,

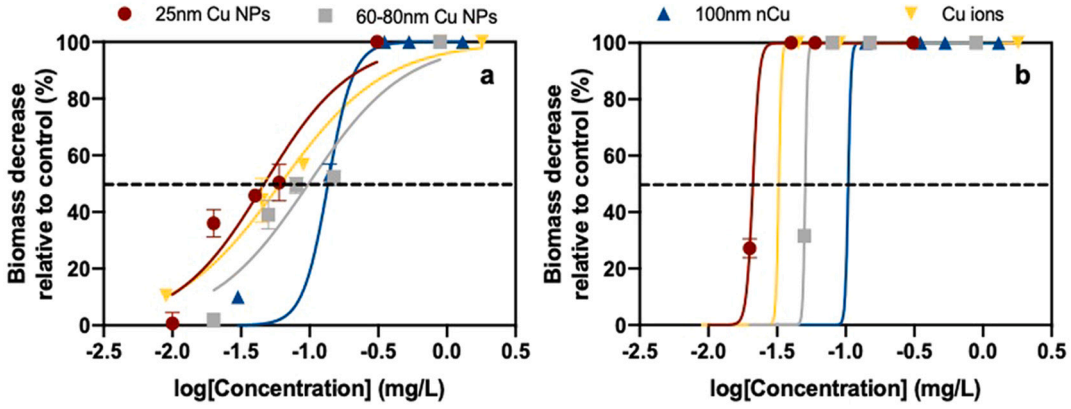

Fig. 5. Dose-response curves of fresh biomass decrease of *Lactuca sativa* L exposed to suspensions of Cu $NPs_{(total)}$ and solutions of $Cu(NO_3)_2{\cdot}2H_2O$ for 144 (a) and 480 h (b) of exposure. Exposure concentrations are expressed as the time weighted average concentrations. Data represent the mean ± SD (n = 3).

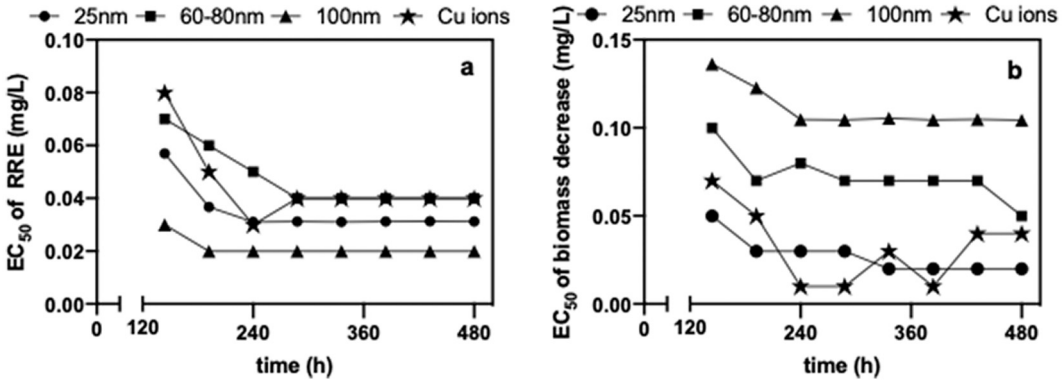

Fig. 6. EC_{50} of RRE (a) and fresh biomass decrease (b) of *Lactuca sativa* L exposed to suspensions of Cu $NPs_{(total)}$ and $Cu(NO_3)_2{\cdot}2H_2O$ after 144 h to 480 h exposure. The EC_{50}-values are expressed as time weighted average concentrations.

confirming the results of Echavarri-Bravo et al. (2015) of negative impacts of NPs on plant growth. No obvious size-effect was observed for either RRE or biomass production (Table 2). The size-effect of NPs has previously been described with daphnids (Lopes et al., 2014), algae (Aruoja et al., 2009) and bacteria (Simon-Deckers et al., 2009). Hua et al. (2014) observed a linear increase of the LC_{50}-values for the impacts of Cu-NPs with sizes ranging from 25 to 100 nm on lethality to zebrafish embryos. In the present study a similar trend was only observed for the specific case of the impact of suspensions Cu NPs on biomass production (Table 2).

Industrially relevant nanomaterials such as TiO_2, CeO_2 and $BaSO_4$ have been classified as being poorly soluble particles with low toxicity (Borm and Driscoll, 2019). The results of our study confirm the classification for $BaSO_4$. It was shown that the extent of ion release from the $BaSO_4$ NPs was low (<1% of the total concentration) and neither the particles nor the ions exerted any toxic effects to plants, even at concentrations of up to 1000 mg L^{-1}. This finding is not in line with the results of the research of Suwa et al. (2008) as these authors considered the barium ion to be the driving force for the observed toxic effects on inhibition of growth of soybean plants with 5 mmol of Ba ions shutting down stomatal openings and perturbing the carbon fixation metabolism and carbon translocation. On the other hand, Lamb et al. (2013) reported negligible uptake of Ba^{2+}-ions after exposing spinach to extracts of barite contaminated soil and these authors indicated that adverse effects to either plants (exposure via soil) or to children after consumption of barium containing plants, is unlikely to cause adverse effects. The solubility of Barium is the key factor concerning its ecotoxicity: toxicity studies with $BaSO_4$ in the form of 100% barite have reported no obvious indications of toxicity, and even no significant differences in biological response were observed at the highest doses (>106 mg kg^{-1} soil). These observations, combined with the observation of lack of toxicity at all doses of $BaSO_4$ nanoparticles with a diameter of 100 nm imply in our opinion that adverse effects are unlikely to occur for $BaSO_4$ particles of size >100 nm. The kinetics of dissolution increase upon decreasing particle size and this is why our findings cannot be directly extrapolated to smaller sized particles. However, the observed lack of toxicity of Ba^{2+} is indicative of a lack of toxicity of smaller sized $BaSO_4$-nanoparticles. Taken together, our results confirmed the general findings of Lamb et al. and showed that the particulate as well as the ionic form of $BaSO_4$ NPs did not exert any effects on the growth of lettuce plants, independent of the endpoint assessed.

With regard to similarity assessment of NFs, the results of this case study clearly show that it is not possible to group NFs of different chemical composition. On the basis of the dose-response curves and the resulting EC_{50} values of the differently sized Cu NPs reported in Table 2 it can on the other hand be concluded that for the endpoints of RRE and biomass production of lettuce seedlings it is indeed possible to group spherical Cu NFs of particle diameter in between 25 and 100 nm. As there is little variation amongst the reported EC_{50}-values and as there is no clear indication of any correlation between particle size and toxicity, it can be concluded that the set of Cu NFs is indeed similar and all information available on any of the NFs within the group, can only be applied to the specific NFs when considering the tested endpoints (RRE and biomass production). In addition, data available on Cu^{2+}-ion toxicity can be used to fill in the data requirements for the risk assessment of similar spherical Cu NFs.

5. Conclusions

The key aims of this case study were to exemplify the integration of fate and effect assessment to assess in order to perform similarity assessment of a set of spherical NPs of different chemical composition and particle. It is to be concluded that for similarity assessment of soluble and non-soluble NPs the time weighted average particle or ion concentrations are proper means of incorporating the fate of either particles and ions on the dose-response relationships obtained for the NFs studied. Chemical composition is shown to determine the fate and subsequently the toxicity of the NFs. The hypotheses of higher ion release occurring for lower-sized NFs and ionic toxicity to be the dominant contributor to the total toxicity of suspensions of NPs were shown to be incorrect and no relationship between NF size and NF toxicity for the endpoints root elongation and biomass production of lettuce were found. For the purpose of similarity assessment of spherical Cu NFs, data on the tested Cu NF with nominal size in between 25 and 100 nm can be used for the risk assessment of specific Cu NF within this size range but with the endpoint considered.

Declaration of Competing Interest

The authors declare that they have no known competing financial interests or personal relationships that could have appeared to influence the work reported in this paper.

Acknowledgements

This work was supported by the GRACIOUS project that is part of the European Union's Horizon 2020 research and innovation programme [grant number 760840]. The Chinese Scholarship Council (CSC) is gratefully acknowledged for its financial support to Yuchao Song (201906320061). We also greatly acknowledge the Nanomaterials Repository of the Joint Research Centre (JRC) of the European Union (Ispra, Italy) for providing the $BaSO_4$ NPs.

Appendix A. Supplementary data

Supplementary data to this article can be found online at https://doi.org/10.1016/j.impact.2022.100397.

References

Abbas, Q., Yousaf, B., Ullah, H., Ali, M.U., Ok, Y.S., Rinklebe, J., 2020. Environmental transformation and nanotoxicity of engineered nanoparticles (ENPs) in aquatic and terrestrial organisms. Crit. Rev. Environ. Sci. Technol. 50, 2523–2581.

Adeleye, A.S., Conway, J.R., Perez, T., Rutten, P., Keller, A.A., 2014. Influence of extracellular polymeric substances on the long-term fate, dissolution, and speciation of copper-based nanoparticles. Environ. Sci. Technol. 48, 12561–12568.

Angel, B.M., Batley, G.E., Jarolimek, C.V., Rogers, N.J., 2013. The impact of size on the fate and toxicity of nanoparticulate silver in aquatic systems. Chemosphere 93, 359–365.

Arenas-Lago, D., Monikh, F.A., Vijver, M.G., Peijnenburg, W.J., 2019. Dissolution and aggregation kinetics of zero valent copper nanoparticles in (simulated) natural surface waters: simultaneous effects of pH, NOM and ionic strength. Chemosphere 226, 841–850.

Arts, J., Hadi, M., Keene, A.M., et al., 2014. A critical appraisal of existing concepts for the grouping of nanomaterials. Regul. Toxicol. Pharmacol. 70 (2), 492–506.

Aruoja, V., Dubourguier, H.C., Kasemets, K., Kahru, A., 2009. Toxicity of nanoparticles of CuO, ZnO and TiO2 to microalgae Pseudokirchneriella subcapitata. Sci. Total Environ. 407, 1461–1468.

Baalousha, M., Cornelis, G., Kuhlbusch, T., Lynch, I., Nickel, C., Peijnenburg, W., Van den Brink, N., 2016. Modeling nanomaterials fate and uptake in the environment: current knowledge and future trends. Environ. Sci. Nano 3, 323–345.

Ban, Z., Zhou, Q., Sun, A., Mu, L., Hu, X., 2018. Screening priority factors determining and predicting the reproductive toxicity of various nanoparticles. Environ. Sci. Technol. 52, 9666–9676.

Borm, P.J., Driscoll, K.E., 2019. The hazards and risks of inhaled poorly soluble particles–where do we stand after 30 years of research? Particle and Fibre Toxicol. 16, 1–5.

Chen, Z., Meng, H., Xing, G., Chen, C., Zhao, Y., Jia, G., Wang, T., Yuan, H., Ye, C., Zhao, F., Chai, Z., 2006. Acute toxicological effects of copper nanoparticles in vivo. Toxicol. Lett. 163, 109–120.

Conway, J.R., Adeleye, A.S., Gardea-Torresdey, J., Keller, A.A., 2015. Aggregation, dissolution, and transformation of copper nanoparticles in natural waters. Environ. Sci. Technol. 49, 2749–2756.

European Union, Commission Regulation (EU) 2018/1881 of 3 December 2018 amending Regulation (EC) No 1907/2006 of the European Parliament and of the Council on the Registration, Evaluation, Authorisation and Restriction of Chemicals (REACH) as regards Annexes I, III, VI, VII, VIII, IX, X, XI, and XII to address nanoforms of substances (Text with EEA relevance.) in C/2018/7942, Brussels, 2018.

Hedberg, J., Blomberg, E., Odnevall Wallinder, I., 2019. In the search for nanospecific effects of dissolution of metallic nanoparticles at freshwater-like conditions: a critical review. Environ. Sci. Technol. 53, 4030–4044.

Hortin, J.M., Anderson, A.J., Britt, D.W., Jacobson, A.R., McLean, J.E., 2020. Copper oxide nanoparticle dissolution at alkaline pH is controlled by dissolved organic matter: influence of soil-derived organic matter, wheat, bacteria, and nanoparticle coating. Environ. Sci. Nano 7, 2618–2631.

Hua, J., Vijver, M., Ahmad, F., Richardson, M., Peijnenburg, W., 2014. Toxicity of different-sized copper nano- and submicron particles and their shed copper ions to zebrafish embryos. Environ. Toxicol. Chem. 33, 1774–1782.

Konate, A., Wang, Y., He, X., Adeel, M., Zhang, P., Ma, Y., Ding, Y., Zhang, J., Yang, J., Kizito, S., Rui, Y., 2018. Comparative effects of nano and bulk-Fe_3O_4 on the growth of cucumber (Cucumis sativus). Ecotoxicol. Environ. Saf. 165, 547–554.

Lamb, D.T., Matanitobua, V.P., Palanisami, T., Megharaj, M., Naidu, R., 2013. Bioavailability of barium to plants and invertebrates in soils contaminated by barite. Environm. Sci. Techn. 47, 4670–4676.

Lin, Y., Allen, H.S., di Toro, D.M., 2018. Validation of Cu toxicity to barley root elongation in soil with the Terrestrial Biotic Ligand Model developed from sand culture. Ecotoxicol. Environ. Safety 148, 336–345.

Liu, Y., Baas, J., Peijnenburg, W.J., Vijver, M.G., 2016. Evaluating the combined toxicity of cu and ZnO nanoparticles: utility of the concept of additivity and a nested experimental design. Environm. Sci. Techn. 50, 5328–5337.

Lopes, S., Ribeiro, F., Wojnarowicz, J., Łojkowski, W., Jurkschat, K., Crossley, A., Soares, A.M.V.M., Loureiro, S., 2014. Zinc oxide nanoparticles toxicity to Daphnia magna: size-dependent effects and dissolution. Environ. Toxicol. Chem. 33, 190–198.

Lv, Z., Sun, H., Du, W., Li, R., Mao, H., Kopittke, P.M., 2021. Interaction of different-sized ZnO nanoparticles with maize (Zea mays): accumulation, biotransformation and phytotoxicity. Sci. Total Environ. 148927.

Misra, S.K., Dybowska, A., Berhanu, D., Luoma, S.N., Valsami-Jones, E., 2012. The complexity of nanoparticle dissolution and its importance in nanotoxicological studies. Sci. Total Environ. 438, 225–232.

Pedruzzi, D.P., Araujo, L.O., Falco, W.F., Machado, G., Casagrande, G.A., Colbeck, I., Lawson, T., Oliveira, S.L., Caires, A.R., 2020. ZnO nanoparticles impact on the photosynthetic activity of *Vicia faba*: effect of particle size and concentration. NanoImpact 19, 100246.

Peijnenburg, W., Baalousha, M., Chen, J., Chaudry, Q., Von der Kammer, F., Kuhlbusch, T., Lead, J., Nickel, C., Quik, J., Renker, M., Wang, Z., Koelmans, A., 2015. A review of the properties and processes determining the fate of engineered nanomaterials in the aquatic environment. Crit. Rev. Environ. Sci. Technol. 45, 2084–2134.

Pu, S., Yan, C., Huang, H., Liu, S., Deng, D., 2019. Toxicity of nano-CuO particles to maize and microbial community largely depends on its bioavailable fractions. Environ. Pollut. 255, 113248.

Simeone, F.C., Blosi, M., Ortelli, S., Costa, A.L., 2019. Assessing occupational risk in designs of production processes of nano-materials. NanoImpact 14, 100149.

Simon-Deckers, A., Loo, S., Mayne-L'hermite, M., Herlin-Boime, N., Menguy, N., Reynaud, C., Gouget, B., Carrière, M., 2009. Size-, composition- and shape-dependent toxicological impact of metal oxide nanoparticles and carbon nanotubes toward bacteria. Environ. Sci. Technol. 43 (21), 8423–8429. https://doi.org/10.1021/es9016975.

Sizochenko, N., Mikolajczyk, A., Syzochenko, M., Puzyn, T., Leszczynski, J., 2021. Zeta potentials (ζ) of metal oxide nanoparticles: a meta-analysis of experimental data and a predictive neural networks modeling. NanoImpact 22, 100317.

Song, C., Huang, M., White, J.C., Zhang, X., Wang, W., Sarpong, C.K., Jamali, Z.H., Zhang, H., Zhao, L., Wang, Y., 2020. Metabolic profile and physiological response of cucumber foliar exposed to engineered MoS_2 and TiO_2 nanoparticles. NanoImpact 20, 100271.

Sturikova, H., Krystofova, O., Huska, D., Adam, V., 2018. Zinc, zinc nanoparticles and plants. J. Hazard. Mater. 349, 101–110.

Suwa, R., Jayachandran, K., Nguyen, N.T., Boulenouar, A., Fujita, K., Saneoka, H., 2008. Barium toxicity effects in soybean plants. Arch. Environ. Contam. Toxicol. 55, 397–403.

Velicogna, J.R., Schwertfeger, D.M., Beer, C., Jesmer, A.H., Kuo, J., Chen, H., Scroggins, R.P., Princz, J.I., 2020. Phytotoxicity of copper oxide nanoparticles in soil with and without biosolid amendment. NanoImpact 17, 100196.

Wu, J., Wang, G., Vijver, M.G., Bosker, T., Peijnenburg, W.J., 2020a. Foliar versus root exposure of AgNPs to lettuce: Phytotoxicity, antioxidant responses and internal translocation. Environ. Pollut. 261, 114117.

Wu, J., Yu, Q., Bosker, T., Vijver, M.G., Peijnenburg, W.J., 2020b. Quantifying the relative contribution of particulate versus dissolved silver to toxicity and uptake kinetics of silver nanowires in lettuce: impact of size and coating. Nanotoxicology 14, 1399–1414.

Xiao, Y., Vijver, M.G., Chen, G., Peijnenburg, W., 2015. Toxicity and accumulation of Cu and ZnO nanoparticles in Daphnia magna. Environ. Sci. Technol. 49, 4657–4664.

Zhai, Y., Hunting, E., Wouters, M., Peijnenburg, W., Vijver, M., 2016. Silver nanoparticles, ions, and shape governing soil microbial functional diversity: Nano shapes micro. Front. Microbiol. https://doi.org/10.3389/fmicb.2016.01123.

Zhai, Y., Hunting, E.R., Wouterse, M., Peijnenburg, W.J., Vijver, M.G., 2017. Importance of exposure dynamics of metal-based nano-ZnO, -cu and-Pb governing the metabolic potential of soil bacterial communities. Ecotoxicol. Environ. Saf. 145, 349–358.

Zhai, Y., Liu, G., Bosker, T., Baas, E., Peijnenburg, W.J., Vijver, M.G., 2019. Compositional and predicted functional dynamics of soil bacterial community in response to single pulse and repeated dosing of titanium dioxide nanoparticles. NanoImpact 16, 100187.

Zhu, Y., Xu, F., Liu, Q., Chen, M., Liu, X., Wang, Y., Sun, Y., Zhang, L., 2019. Nanomaterials and plants: positive effects, toxicity and the remediation of metal and metalloid pollution in soil. Sci. Total Environ. 662, 414–421.